



Short communication

Development and characterization of a bilayer separator for lithium ion batteries

Xiaosong Huang*

Chemical Sciences & Materials Systems Lab, GM Global R&D, 30500 Mound Rd, Warren, MI 48090, USA

ARTICLE INFO

Article history:

Received 19 April 2011

Received in revised form 17 May 2011

Accepted 19 May 2011

Available online 27 May 2011

Keywords:

Ceramic separator

Coating

Thermal performance

High rate capability

Lithium ion battery

ABSTRACT

A battery separator is placed between the positive and negative electrodes to prevent electric contact of the electrodes while maintaining good ionic flow. The most commonly used separators for lithium-ion batteries are porous polyolefin membranes. However, they generally do not have good dimensional stability at elevated temperatures. In this study, a bilayer separator has been formed directly on an anode. This bilayer separator comprised a ceramic layer and a porous polyvinylidene fluoride (PVDF) layer. Coin cells with this type of separators showed stable cycling performance at room temperature. They also showed significantly improved rate capabilities compared to the reference cell with a conventional polyolefin separator. An oven test has been used to characterize the cells thermal stability. Charged cells were kept in an oven at 150 °C and their voltage drop was recorded. The reference cell with a conventional separator failed within about 50 min, while no noticeable voltage drop was observed for the cells with the new bilayer separator within the measured 2 h.

© 2011 Elsevier B.V. All rights reserved.

1. Introduction

The application of lithium-ion (Li-ion) batteries has been expanding from consumer electronics to industrial usage including plug in electric vehicles (PEVs) and hybrid electric vehicles (HEVs). Intensive research has been conducted to increase the energy and power densities, reduce the cost, and improve the abuse tolerance of the batteries [1–3].

A separator is a critical component of a Li-ion battery [4,5]. It separates the positive and negative electrodes and enables the ionic conductivity through the liquid electrolyte filled in its porous structure. Polyolefin microporous membranes are the most commonly used separators for Li-ion batteries. However, without surface treatment, microporous polyolefin separators have low wettability by the electrolyte [6,7]. Furthermore, these polyolefin membranes will shrink, soften, and even melt as the temperature reaches 130 °C or higher. This could cause internal short circuits, leading to battery thermal runaway. Therefore, a separator that does not shrink or melt at elevated temperatures becomes desirable.

Ceramic separators have attracted increasing attention as they can provide excellent thermal stability and good wettability by the liquid electrolyte [8–10]. Due to the high compact strength of ceramic particles, ceramic separators are also very resistant to dendrite penetration so to significantly reduce the risk of electric short. Ceramic separators are membranes of ceramic particles bound by

a polymeric binder. As an effort to reduce the separator production cost ceramic separators have been formed on electrodes directly [11–13]. However, the direct coating of ceramic particles has some drawbacks, such as particle loss, brittleness, and low air permeability.

Polyvinylidene fluoride (PVDF) is well known to the battery community as it has been widely used as gel polymer electrolytes and electrode binders in Li-ion batteries. Porous PVDF membranes have also been investigated as battery separators [14–17]. This polymer can be made into a free standing film or coated directly on an electrode through a phase inversion process [14–17]. PVDF separators can enable good ionic conductance, but suffer from low thermal stability above 150 °C in an electrolyte. In addition, they are normally less tolerant of short (e.g., dendrite issues) as their mechanical properties (elastic and shear moduli) are too low to prevent dendrite formation and penetration.

In this work, a bilayer composite separator was developed. A ceramic layer was first coated on the anode to provide functions such as high thermal stability and dendrite penetration resistance to the battery. A porous PVDF layer was then formed on the top of the ceramic layer to provide good adhesion to the counter electrode. Good adhesion to electrodes can decrease the interfacial impedance and reduce the chance of lithium dendrite formation upon overcharge and overdischarge [18,19]. The porous PVDF layer also played an important role in buffering the electrode volume change during the charge–discharge cycle. In addition, it kept the ceramic particles from dropping during cell fabrication. The porous PVDF was formed through a solvent evaporation induced phase inversion process.

* Tel.: +1 586 9860836; fax: +1 586 9861207.

E-mail address: xiaosong.huang@gm.com

2. Materials and experiments

2.1. Materials

Polyvinylidene fluoride (PVDF) was provided by Arkema Inc. (Philadelphia, PA) under the product name of Kynar® 761. Polyacrylonitrile (PAN) and analytical grade dimethylformamide (DMF) were purchased from Sigma–Aldrich (St. Louis, MO). Silica powder used in this work was a ground, natural crystalline silica with at least 99.2% SiO₂. Analytical grade acetone was purchased from Mallinckrodt Chemicals (St. Louis, MO).

The cathode material used in this work was LiNi_{1/3}Co_{1/3}Mn_{1/3}O₂ (Toda NCM-01ST-100) (NCM). The anode material was TIMREX SLP 30 graphite. TIMREX Super P Li carbon black was used in electrode formulation as the conductive additive. Kynar HSV 900 PVDF (Arkema Inc., Philadelphia, PA) was used as the binder for the electrode materials.

2.2. Experiments

The cathode was prepared by spreading a slurry of cathode ingredients in N-methylpyrrolidone (NMP) on an aluminum current collector of 20 μm thick, followed by drying at 100 °C for 12 h. The weight ratio of NCM/carbon black/PVDF in the cathode formulation was 90/6/4. The anode was prepared in a similar procedure. The collector used was a 20 μm copper foil. The electrode composition was 90 wt.% graphite, 6 wt.% carbon black and 4 wt.% binder.

To prepare the dispersion for the ceramic coating, 1 g of PAN was dissolved in 100 g of DMF at 50 °C to form a 1 wt.% solution. Into this solution, 65 g of dried silica powder was added under vigorous mechanical stirring to form a uniform dispersion. The silica dispersion was used to form the ceramic layer in the bilayer separator coating.

The solution for the PVDF coating was formed as following. Six grams of PVDF was dissolved in 90 g of acetone at 50 °C. Three grams of water was then added into the PVDF solution. The mixture was stirred at 50 °C till a uniform solution was formed.

To form the bilayer separator, the silica dispersion was coated on the surface of the graphite anode by a doctor blade. The coating thickness was adjusted so that the dried coating was about 20 μm thick. Once the ceramic coating was partially dried at 80 °C for 4 min, the PVDF coating was applied. The PVDF solution was spread on the ceramic coated electrode with a doctor blade. The coating was then dried at 60 °C for 2 h.

For comparison, a single porous PVDF layer was coated directly on the electrode. The PVDF solution was spread on the electrode to form a porous coating as described in the previous case for the formation of the porous PVDF layer in the bilayer separator. The thickness of the applied PVDF solution was adjusted so that the formed porous membrane was about 25 μm.

The separator coated electrode was fractured in liquid nitrogen and its fracture surface was observed by scanning electron microscope (SEM).

The porosities of the ceramic and PVDF layers were estimated by forming the two layers on a flat surface separately, measuring the thicknesses and weights of the dried layers, and calculating their porosities based on the densities of PVDF and ceramic particles using the equation below.

$$P = 1 - \frac{w_T}{\rho \cdot V_a}$$

where w_T is the weight of the dry membrane, ρ is the density of the membrane material (ceramic or PVDF), and V_a is the apparent volume of the membrane.

Ionic conductivity is a material property. In order to compare the separator performance, effective ionic conductivity of the inter-

electrode medium (separator saturated with a liquid electrolyte) has been used in this work. It was calculated from the following equation:

$$\sigma = \frac{d}{R_b \cdot S} = \frac{1}{\rho}$$

where d is the thickness of the film, R_b is the bulk resistance, and S is the area of the electrode. The membrane was filled with a liquid electrolyte (1.1 M LiPF₆ in ethylene carbonate (EC)/dimethyl carbonate (DMC) (1/1 by volume)) and sandwiched between two stainless steel electrodes. R_b was obtained using an impedance analyzer.

CR2325-type coin cells were prepared to evaluate the electrochemical performance of the cells with different types of separators. Coin cells were assembled with the NCM electrode as the cathode, graphite as the anode, and 1 M LiPF₆ in ethylene carbonate (EC)/diethyl carbonate (DEC) (1:2 by volume) as the electrolyte. Cells with a Celgard polypropylene separator were also prepared. Battery tests such as cycle life and rate capability were carried out on a Maccor Series 4000 battery tester at 30 °C. The CR2325-type coin cells were charged up to 4.3 V under a constant current–constant voltage mode, and then discharged to 3.0 V under a constant current mode. For the cycle test, cells were charged at C/5 rate and discharged at C/5 rate in the first 5 cycles and C/2 rate in the following cycles. As for the rate capability test, cells were charged at C/5 rate and discharged at C/5, C/2, 1C, 2C, 4C, and 8C rates.

In order to investigate separator thermal stability, an accelerating rate calorimeter (ARC® from Netzsch) was used to measure the cell voltage response at an elevated temperature. Cells were charged to 4.3 V and then placed in the ARC vessel capable of heating to a desired temperature. The cell skin temperature was maintained at 150 °C and cell open circuit voltage was recorded.

3. Results and discussion

Hereinafter, the single layer PVDF separator and the bilayer composite separator are referred to as C1 and C2, respectively. Fig. 1 shows the cross-section of the anode coated with C2. C2 had two layers. The first (or bottom) layer of about 22 μm thick was comprised of ceramic particles. A certain amount of ceramic particles are needed to ensure a uniform pore-size distribution. The second (or top) layer was a porous PVDF coating of about 6 μm thick. PVDF layer protects the ceramic particles from falling off the electrode, flatten the coating surface, and improve the adhesion to the counter electrode. The porous structure in this work was formed via a preferential evaporation process. The evaporation of the solvent acetone at room temperature resulted in increased concentrations of both PVDF and non-solvent water. Phase separation was then followed by forming a polymer rich and a polymer lean phase. When water was evaporated at 60 °C, pores were formed at the locations where the polymer lean phase had existed. As seen in the figure, the PVDF layer had a uniform porous structure.

Appropriate separator porosity is necessary since too low a porosity does not provide good inter-electrode ionic conductance while too high a porosity can lead to an increased risk of electrical shorting by particulates or dendrites. The typical porosity for commercialized lithium-ion battery separators is about 40–50%. Table 1 shows the calculated porosities of C1 and C2. Despite the high ceramic content, foldable membranes were obtained for the porosity test. C1 had a porosity of about 68%, which is much higher than that of a commercial polyolefin separator. The ceramic layer and the PVDF layer in C2 had porosities of about 39% and 65%, respectively.

Effective ionic conductivity results are listed in Table 2. Both C1 and C2 enabled higher effective ionic conductivities compared

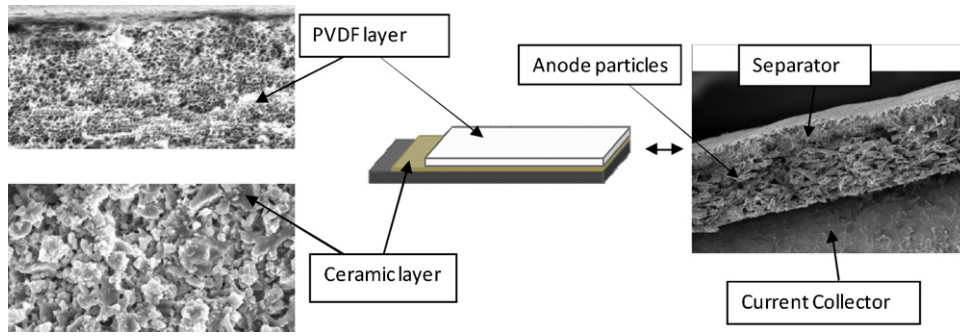


Fig. 1. SEM photographs of the cross-section of the anode coated with C2.

Table 1
Thicknesses and porosities of C1 and C2.

		C1	C2
Thickness (μm)	Layer 1	27	22
	Layer 2	6	6
Porosity (%)	Layer 1	68	39
	Layer 2		65

to a commercial polypropylene separator. The high porosity and the capability for PVDF to form a gel electrolyte contributed to the good ionic conductance when C1 was tested. The high porosity and the excellent wettability of the ceramic particles by the liquid electrolyte led to the high effective ionic conductivity of the liquid electrolyte saturated C2.

The separator performance was evaluated through testing the electrochemical and thermal properties of CR2325-type coin cells. Cells with the conventional polypropylene separator, C1, and C2 were fabricated. Fig. 2a shows the cell cycle performance. At 30 °C, all the graphite/NCM cells showed stable cyclability. The capacity retention ratios of the cells with C1 and C2 were about 86% at the end of the first 50 cycles. Compared with the 82% capacity retention for the cell with the conventional polypropylene separator, they provided better cycle performance. The profiles for the first charge–discharge cycles are shown in Fig. 2b. All the cells showed similar columbic efficiencies of about 79%. With an increase in the cycle number, the columbic efficiency of each charge and discharge cycle gradually reached 100%. Unstable voltage profiles were not observed for cells with C1 and C2. The stable voltage profiles would be ascribed to the small pore-size and narrow pore-size distribution [10].

Fig. 3 shows rate capabilities of cells with different separators. The y-axis indicates the capacity retention ratio calculated by dividing the discharge capacity of the n th cycle by the discharge capacity of the first cycle. Cells with different separators showed similar capacity retentions at C/5 rate. Their discharge capacities decreased gradually with the increase in C-rate, which reflects the polarization. It is evident that cells with C1 and C2 separators showed higher capacity retentions at high rates (i.e. 1C, 2C, 4C, and 8C) compared to the cell with the conventional polypropylene separator. The cell with the conventional polypropylene separator showed an abrupt decrease in capacity retention when increasing the C-rate to 4C and 8C. Its capacity retention ratios at 4C and 8C were about 55%

Table 2
Effective ionic conductivities of the membranes saturated with a liquid electrolyte.

Sample	Effective conductivity (mS cm^{-1})
Polypropylene separator	0.94
C1	1.72
C2	1.57

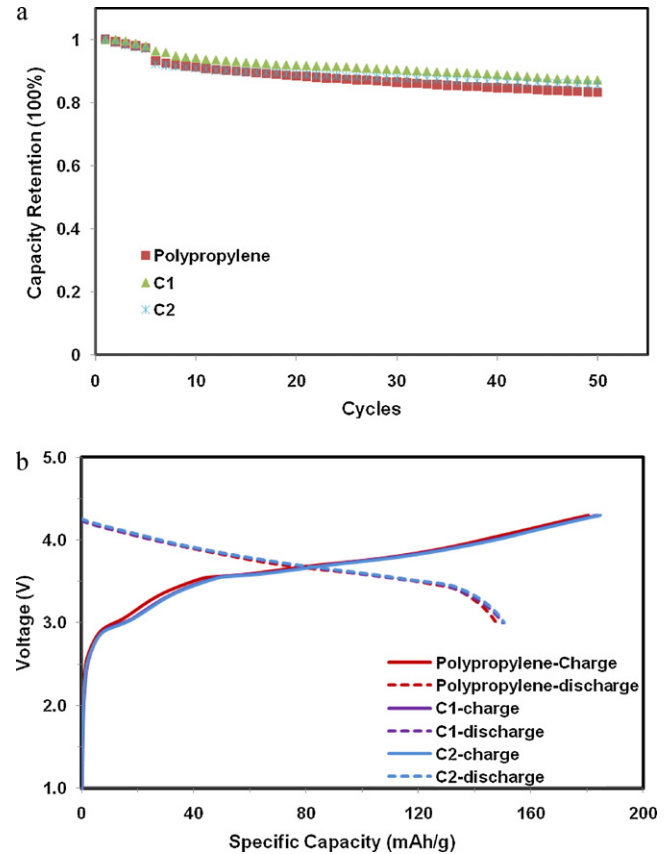


Fig. 2. (a) Cycle performance of cells with the conventional polypropylene separator, C1, and C2; (b) first cycles of the charge–discharge profiles of cells with different separators.

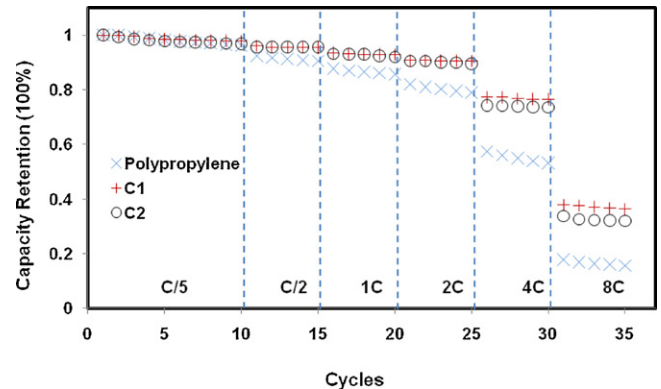


Fig. 3. Rate capability test of the cells with different separators.

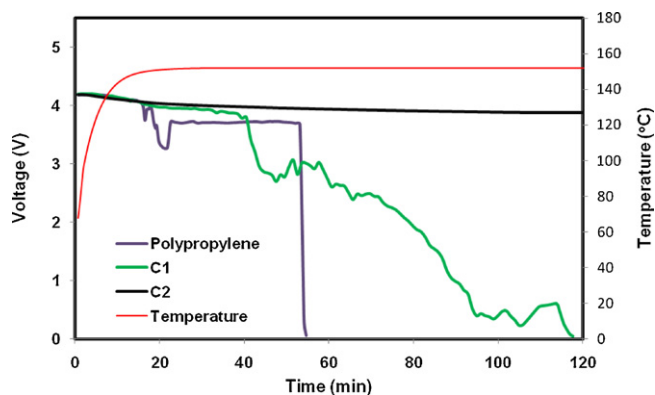


Fig. 4. Open circuit voltage profiles for cells with different separators.

and 16%, respectively. However, the cells with C1 and C2 showed higher discharge capacities. The capacity retention ratios at 4C and 8C were about 77% and 38%, respectively, for the cell with C1 and about 73% and 32%, respectively, for the cell with C2. The good rate performance is an indication of a low internal polarization due to the high inter-electrode ionic conductance of the cells with C1 and C2 and/or the low interfacial contact resistances between the electrodes and C1/C2. The cell with C1 showed better rate performance compared to the cell with C2, which can be attributed to the higher porosity in C1.

Cell thermal performance was evaluated through a hot oven test using ARC. Cells were kept in the heating vessel at 150 °C to induce internal short. A short develops when conductive particulate bridge the separator or the separator itself deteriorates to the point where it allows the positive and negative electrodes to touch. Internal short circuits are evidenced by precipitous drops in cell voltage. Results of the hot oven tests are given in Fig. 4. The cell with the conventional polypropylene separator showed sudden voltage drop after 50 min from the start of the test. The voltage drop was probably caused by the internal short circuit due to the thermal shrinkage of the separator. Polyolefin separators are usually stretched at elevated temperatures during manufacturing to enlarge porosity. The conventional polypropylene separator showed a shrinkage of about 25% in the stretching direction (or machine direction) when maintained at about 150 °C for 1 h. The cells with C1 showed a slow cell voltage decrease starting at about 40 min after the start of the test. The slow voltage drop generally indicates a “soft short”, which is mostly induced by the formation of small localized contact between electrodes. At elevated temperatures, the gel polymer electrolyte (porous PVDF) usually becomes very weak or even fluid given a sufficient amount of liquid electrolyte [18]. Electrode particles can penetrate the PVDF layer relatively easily, especially when an external pressure is applied. The “soft short” was probably due to the local conductive path formed by the electrode particles. On the other hand, the cell with C2 showed a very gentle voltage drop, and no sudden voltage change was observed during the hot oven

test in up to 2 h. This result suggests C2 is thermally stable in the liquid electrolyte so to protect the cell from internal short at the high temperature of 150 °C.

4. Conclusions

A separator comprising a ceramic layer and a porous polyvinylidene fluoride (PVDF) was formed on an anode through a solution casting process. Separator performance was evaluated by building coin cells with $\text{LiNi}_{1/3}\text{Co}_{1/3}\text{Mn}_{1/3}\text{O}_2$ as the cathode, graphite as the anode, and 1 M LiPF_6 in ethylene carbonate (EC)/diethyl carbonate (DEC) (1:2 by volume) as the electrolyte. Cells with this bilayer composite separator showed stable cycling performance at room temperature. The coin cell with this bilayer separator also showed excellent rate capability. At an 8C discharge rate, its capacity retention was about 32%, while the capacity retention of the cell with a commercial separator was only about 16%. The ceramic layer in the bilayer separator enabled a high thermal stability. Cell thermal stability was evaluated by keeping the charged cells at 150 °C and recording their voltage drop. The cell with the conventional polypropylene separator showed a sudden voltage drop in about 50 min. However, only a very gentle voltage drop was observed for the cell with the bilayer separator within the duration of the 2 h test.

Acknowledgments

The author would like to thank Drs. Yan Wu and Hamid Kia at GM for helpful discussions.

References

- [1] M.S. Whittingham, *Chem. Rev.* 104 (2004) 4271–4302.
- [2] M.S. Wu, P.C.J. Chiang, *Electrochim. Acta* 52 (2007) 3719–3725.
- [3] S.S. Zhang, *J. Power Sources* 164 (2007) 351–364.
- [4] X. Huang, *J. Solid State Electrochem.* 15 (2011) 649–662.
- [5] Y.B. He, Q. Liu, Z.Y. Tang, Y.H. Chen, Q.S. Song, *Electrochim. Acta* 52 (2007) 3534–3540.
- [6] J. Saunier, F. Alloin, J.Y. Sanchez, G. Caillon, *J. Power Sources* 119–121 (2003) 454–459.
- [7] Y.M. Lee, J.W. Kim, N.S. Choi, J.A. Lee, W.H. Seol, J.K. Park, *J. Power Sources* 139 (2005) 235–241.
- [8] S.S. Zhang, K. Xu, T.R. Jow, *J. Power Sources* 140 (2005) 361–364.
- [9] D. Takemura, S. Aihara, K. Hamano, M. Kise, T. Nishimura, H. Urushibata, H. Yoshiyasu, *J. Power Sources* 146 (2005) 779–783.
- [10] T.H. Cho, M. Tanaka, H. Onishi, Y. Kondo, T. Nakamura, H. Yamazaki, S. Tanase, T. Sakaia, *J. Electrochem. Soc.* 155 (2008) A699–A703.
- [11] V. Hennige, C. Hying, G. Horpel, S. Augustin, *US 2005/0221192*.
- [12] M. Yamashita, S. Oki, *US 6287720*.
- [13] J. Kim, W. Han, J. Min, *US 7659036*.
- [14] S.S. Zhang, K. Xu, D.L. Foster, M.H. Ervin, T.R. Jow, *J. Power Sources* 125 (2004) 114–118.
- [15] A. Du Pasquier, P.C. Warren, D. Culver, A.S. Gozdz, G.G. Amatucci, J.M. Tarascon, *Solid State Ionics* 135 (2000) 249–257.
- [16] Q. Shi, M.X. Yu, X. Zhou, Y.S. Yan, C.R. Wan, *J. Power Sources* 103 (2002) 286–292.
- [17] E. Pasquier, *US 6235065*.
- [18] J. Chojnacka, J.L. Acosta, E. Morales, *J. Power Sources* 97–98 (2001) 819–821.
- [19] M. Majima, T. Tada, S. Ujiie, E. Yagasaki, S. Inazawa, K. Miyazaki, *J. Power Sources* 81–82 (1999) 877–881.